The rheology and microstructure of an aging thermoreversible colloidal gel

Melissa B. Gordon, Christopher J. Kloxin, Norman J. Wagner[1]

M. B. Gordon, Prof. C. J. Kloxin, Prof. N. J. Wagner
Department of Chemical and Biomolecular Engineering
Center for Molecular and Engineering Thermodynamics
University of Delaware
150 Academy Street
Newark, DE 19716
USA

Prof. C. J. Kloxin
Department of Material Science and Engineering
University of Delaware
201 DuPont Hall
Newark, DE 19716
USA

Keywords: thermoreversible colloidal gel, aging, gel microstructure, free energy landscape

Abstract

Colloidal gels exhibit time-dependent bulk properties. However, the processes and mechanisms by which aging occurs are poorly understood, which complicates the prediction of macroscopic behavior in these systems. Using a model, thermoreversible, adhesive hard sphere system consisting of octadecyl-coated silica nanoparticles dispersed in tetradecane, rheological aging is quantitatively related to structural aging. By simultaneously measuring the bulk properties and gel microstructure using rheometry and small angle neutron scattering (Rheo-SANS), respectively, we show a one-to-one correspondence between the time-dependent storage modulus and the microstructure, and further, that this correspondence is independent of the gel's thermal and shear history. At the working volume fraction, the gel is homogenous and, unlike phase-separated gels, aging behavior is not due to heterogeneous coarsening. Instead, the results presented here are consistent with homogeneous, local particle rearrangements as the mechanism of rheological aging. By establishing a quantitative and predictive relationship between the underlying microstructure and bulk mechanical properties, the results of this study may be 1) industrially relevant to products that age on commercially-relevant timescales, 2) applicable to other dynamically arrested systems, such as metallic glasses, and 3) valuable in the design of new materials.

[1] Corresponding author: wagnernj@udel.edu

I. Introduction

Understanding the molecular mechanisms underlying macroscopic bulk property changes in colloidal systems provides fundamental insights that transcend many material systems. While this understanding can be exploited to design new advanced materials, it has direct implications on the stability of a wide variety of colloidal-based consumer products, such as pharmaceuticals, food and personal care items. Macroscopic property changes in non-reacting systems result from external triggers to the system (e.g., stress, temperature, gravity) or from the internal dynamical evolution of the system (e.g., aging). Colloidal gels, in particular, exhibit highly complex behavior arising from their fundamentally disordered microscopic structure. These systems are dynamically arrested and have significantly reduced mobility, which prevent the gel from reaching thermodynamic equilibrium on an experimental timescale [1-3]. This non-equilibrium state often gives rise to aging behavior in which the bulk properties are a function of when the material was first quenched (e.g., via temperature or concentration) and change with gel age [1-3]. As a result, macroscopic properties in aging systems are challenging to measure and predict, but are necessary to determine product shelf-life as well as long-term efficacy and safety.

The process and mechanism by which aging occurs is not well understood; however, it is generally accepted that the aging of colloidal gels is governed by their free energy landscape [4, 5]. The free energy landscape directly corresponds to the microstructure of the system such that measurements of structural evolution during aging can be used to validate simulations [6]. From this perspective, the thermodynamic equilibrium state is located in the deepest well, but other free energy minima do exist. The system samples a reduced set of the available configurational space via thermal motion on the timescale of the experiment, which results in time-dependent bulk properties. As the system continues to evolve, it samples lower and lower free energy minima, approaching the global thermodynamic equilibrium. Here, we explore this view of gel aging as a trajectory in a free energy landscape by examining gel microstructure simultaneous with rheology using advanced Rheo-SANS methods [7].

The phenomenon of aging is of both fundamental importance and industrial relevance. As such, it has been investigated in numerous model systems yet, based on this work, it is important to differentiate between aging in homogeneous gels versus phase-separated gels [8]. (For a comprehensive review of colloidal gels, see reference [9].) One such homogeneous model system is the well-studied adhesive hard sphere (AHS) system, which is employed in this study, and consists of silica nanoparticles grafted with an octadecyl brush dispersed in an organic solvent [8, 10-20]. In this system, particle interactions associated with the steric repulsion of the octadecyl brush are tuned by temperature [21]. This system can be fully rejuvenated by thermal cycling; the gel is heated to its liquid state and sheared using a well-established pre-shear protocol to completely erase its structural history. Indeed, Negi et al. studied the gelation of similar systems after shear fluidization and shear cessation, but did not measure microstructural evolution [22]. Eberle et al. observed rheological aging in a homogenous AHS gel consisting of octadecyl-coated silica nanoparticles dispersed in tetradecane; the authors reported a steady increase in the storage modulus in time during a constant frequency, small amplitude oscillatory

shear (SAOS) experiment and postulated that this may be due to the interdigitation of the octadecyl chains [17]. Similarly, Guo and co-workers observed rheological aging and dynamical heterogeneity in a system composed of octadecyl-grafted silica nanoparticles suspended in decalin [2]. They described late stages of aging with a power law relationship between the storage modulus and waiting time, t_w, ($G' \sim t_w^{0.4}$). Importantly, they observed a time-evolving microstructure as measured by x-ray scattering while the gel formed and subsequently aged, but did not quantitatively connect the structural aging to that of the bulk rheological properties.

A fundamentally distinct model system often employed in aging studies is the colloid-polymer depletion gel. In depletion gels, polymer colloids (e.g., polymethylmethacrylate) are dispersed in an organic solvent and a non-adsorbing polymer is added (e.g., polystyrene), which promotes interparticle attraction through depletion forces [23]. Experimental and simulation work suggest that these phase-separated gels coarsen over time, thereby resulting in colloid-rich regions and colloid-poor voids [24-27]. The phase separation results in time-dependent phenomena, such as the 'delayed sedimentation' that Poon and coworkers observed using dark-field imaging of gels composed of PMMA particles and polystyrene [24]. Similarly, delayed collapse due to continuous coarsening was further quantified in the work of Buscall et al. [25]. Verhaegh et al. argued through small angle light scattering measurements and optical microscopy that the gelation was driven by spinodal decomposition of the gel [28]. However, the gel continues to restructure over all lengths scales, which leads to continued phase separation that eventually causes the collapse of the gel. Additionally, Zhang and co-workers investigated the dynamics during phase separation and define two regimes of behavior—classical and viscoelastic—which depend on the polymer concentration and interaction length (i.e. polymer-colloid size ratio) [29]. It is important to note that this model system is highly complex, and one such complication arises from the use of shear to homogenize and rejuvenate these gels. Recently, it has been shown that the shear rate influences the resultant structure and mechanical properties of gels composed of PMMA and polystyrene [30]. Currently, the effect of shear on colloidal gels is not well understood [3] and we provide additional insight on this effect by examining the evolution of gel microstructure under shear in a thermoreversible system. Because this system can be fully rejuvenated via thermal cycling, we can compare thermal cycling to the effect of shear, which may appear to rejuvenate mechanical properties, but not fully restore the gel structure.

In the work presented here, we connect rheological aging with structural aging by concurrently measuring the mechanical properties and microstructure of the gel using rheometry and small angle neutron scattering (Rheo-SANS). In particular, we are especially interested in determining if the aging behavior in an AHS colloidal system is consistent with local particle rearrangements or larger, collective rearrangements within the gel by examining the role of shear history and thermal history on gel formation and aging. For this study, an AHS system consisting of 30 nm silica spheres (volume fraction, ϕ=0.28) with an octadecyl grafted brush dispersed in tetradecane was synthesized. We quench the system just slighly below the gel transition temperature so we can examine aging on an experimentally accessible time scale. At the selected volume fraction, the system is a single-phase, homogeneous gel [17] that does not sediment ($Pe_g << 1$, [31]),

avoiding aging behavior associated with gel coarsening or sedimentation that is observed in phase-separated gels [24-26, 32]. The Rheo-SANS data are analyzed to extract quantitative measures of the evolving microstructure during aging and this is shown to be connected to the evolution of the gel's elasticity. The methods and results presented here should be of industrial relevance for studying a wide range of colloidal systems, including paints, concretes, coatings, inks, and pharmaceuticals, which may exhibit aging behavior on commercially-relevant timescales.

II. Materials and Methods

A. Particle Synthesis

The adhesive hard spheres were synthesized by grafting an octadecyl brush onto 30 nm colloidal silica nanoparticles (Ludox TM-50, Sigma Aldrich) according to the procedure developed by van Helden et al. [10] and further developed by Eberle and co-workers [21]. In brief, the silica suspension was treated with sulfuric acid and then mixed and heated in the presence of 1-octadecanol. The mixture was dissolved in ethanol to graft the brush onto the particle surface via a condensation reaction. The particles were purified by washing three times in a 60/40 mixture of chloroform and cyclohexane using a Sorvall RC 6 Plus centrifuge before drying the particles under a nitrogen stream and finally in a vacuum oven overnight. The particles (ρ=1.80 g/mL) were then dispersed in tetradecane (Fisher, ρ(25°C) =0.7670 g/mL, μ(25°C) = 2.078 mPa s, [33]) at a mass fraction of 0.48, which corresponds to a volume fraction of 0.28, to form a thermoreversible gel. The particles have been characterized extensively using transmission electron microscopy, densitometry, light scattering, rheometry and SANS [17, 21].

B. Rheometry

Rheological measurements were performed on a stress-controlled Discovery Hybrid Rheometer (DHR) from TA Instruments using cone and plate geometry (40 mm cone diameter, 2° cone angle) equipped with a solvent trap and cover. The temperature was controlled using a Peltier plate with a ramp rate of approximately 7°C/min. The sample was fully rejuvenated between tests by applying a pre-shear protocol, where the sample was sheared at a rate of 10 s^{-1} in its liquid state at 40°C for 2 minutes, and then the sample was held quiescently at 40°C for 2 minutes. Full rejuvenation was confirmed by monitoring the viscosity at the conclusion of the pre-shear protocol. All aging experiments were performed at 28.6°C where the sample is a soft gel capable of flowing homogeneously (i.e., without phase separation). Two distinct temperature profiles were used to approach this temperature: 1) quenching from 40°C to 28.6°C (the cooling direction) and 2) quenching from 40°C to 25°C, and then immediately ramping to 28.6°C (the heating direction). Aging experiments were performed within the linear viscoelastic region for the gel at 0.1% strain and 1 Hz. Prior work on this system showed no evidence of shear banding or wall slip [18]. With a solvent trap, the material was stable for approximately 10 days. We note that the gravitational Péclet number is of order 10^{-5}, while the Péclet number for the small amplitude oscillatory shear experiments is of order 10^{-4}. The maximum Péclet number during the shearing at 40°C is also of order 10^{-4}.

C. Rheo-SANS

Simultaneous rheology and small angle neutron scattering (Rheo-SANS) measurements were conducted at the National Institute of Standards and Technology (NIST) Center for Neutron Research (NCNR) in Gaithersburg, MD using the Rheo-SANS sample environment [34]. The sample was loaded in a titanium concentric cylinder geometry with an inner bob diameter of 29 mm and a 0.5 mm gap on an Anton Paar MCR-501 stress-controlled rheometer placed into the NG7 30 m beamline. Time-resolved SANS data was collected in the 1, 3-plane at a detector distance of 13 m with a 15 m lens. The total sample path-length was 1 mm. Transmissions ranged from 0.304 to 0.306 throughout the experiments. Temperature control in this system was imperfect due to slow response (ramp rate of approximately 1°C/min) and overshoot, and therefore cannot be directly compared to temperature ramp data collected on the DHR. As a result, the pre-shear protocol was lengthened; samples were sheared at 10 s^{-1} in its liquid state at 40°C for 10 minutes and then held quiescently at 40°C for 2 minutes. When the heating profile was used, samples were quenched from 40°C to 25°C (for a total of 15 minutes, including the quench) before conducting aging experiments at 28.6°C, 0.1% strain and 1 rad/s. The scattering data was analyzed using the SANS reduction software package available from the NCNR in IGOR Pro [35]. Data was fit to the sticky hard sphere model using the "SmearedPolyCore_SHS" function from the SANS reduction package. Fitting parameters for octadecyl-coated particles are available from the literature [21]. The scattering length density of tetradecane (SLD solvent = -4.4e-07 $Å^{-2}$) was determined from the online NIST scattering length density calculator. The scattering length density of the shell (SLD shell = -3.9e-07 $Å^{-2}$) was determined by fitting the reference state data. The perturbation parameter, which determines the depth of the square-well potential, was set at $\varepsilon = 0.001$ for all cases.

III. Results and Discussion

Concurrent rheometry and time-resolved small angle neutron scattering in an aging gel enables the direct connection between its mechanical property evolution and corresponding microstructure. To obtain mechanistic insight into the causes of the aging behavior, the system was probed by applying varied thermal and shear profiles. In sections IIIA and IIIB, we investigated the mechanical property evolution associated with the formation and aging of a thermoreversible colloidal gel. Specifically, a reproducible reference state (comprised of a temperature and time) was established in the continuously aging gel. Stress was applied to the sample 1) once it has aged to the reference state and 2) before it has reached the reference state (i.e., during its formation). In section IIIC, we support our interpretation of the rheological properties with microstructural measurements and establish a quantitative relationship between the underlying microstructure and the bulk properties during aging.

A. Rheology of an Aging Thermoreversible Gel

In an octadecyl-functionalized colloidal silica system, the interparticle attractions are tuned by temperature. The temporal evolution of the storage (G′) and loss (G″) moduli are monitored in response to a temperature change as shown in Figure 1A. Initially, both moduli are comparable to the instrument's resolution under these test conditions. As the sample is quenched from its

liquid state at 40°C to 28.6°C, both moduli increase by several orders of magnitude, which is associated with the formation of an interacting colloidal gel [8, 17]. Note that the critical gel temperature, corresponding to rigidity percolation, is 28.8°C [36, 37]. After the gel fully forms and the temperature remains constant, the storage and loss moduli continue to increase with time under small amplitude oscillatory shear (SAOS). The continual stiffening of the gel over the experimental timescale is characteristic of rheological aging in these systems [2]. During the gel formation and aging process shown in Figure 1A, the storage modulus dominates the loss modulus and undergoes the greatest change. This time evolution was empirically fit to an error function, which typically describes such diffusive processes, with an induction time as displayed in Figure 1B. The induction time from this empirical fit (parameter D) defines a characteristic time for gel formation to be approximated as ≈270 seconds. This characteristic time is a convolution of the time associated with the temperature quench and gel formation. This characteristic time quantifies the time scale of gel formation following the temperature quench to 28.6°C and demonstrates that significant gel aging occurs long after initial gel formation. Prior work suggested that this characteristic time can be used to scale gelation kinetics in a similar system [22]. We note that this timescale is observational—i.e., it is not fundamental and provides a physical timescale for the process based on the observation method (SAOS).

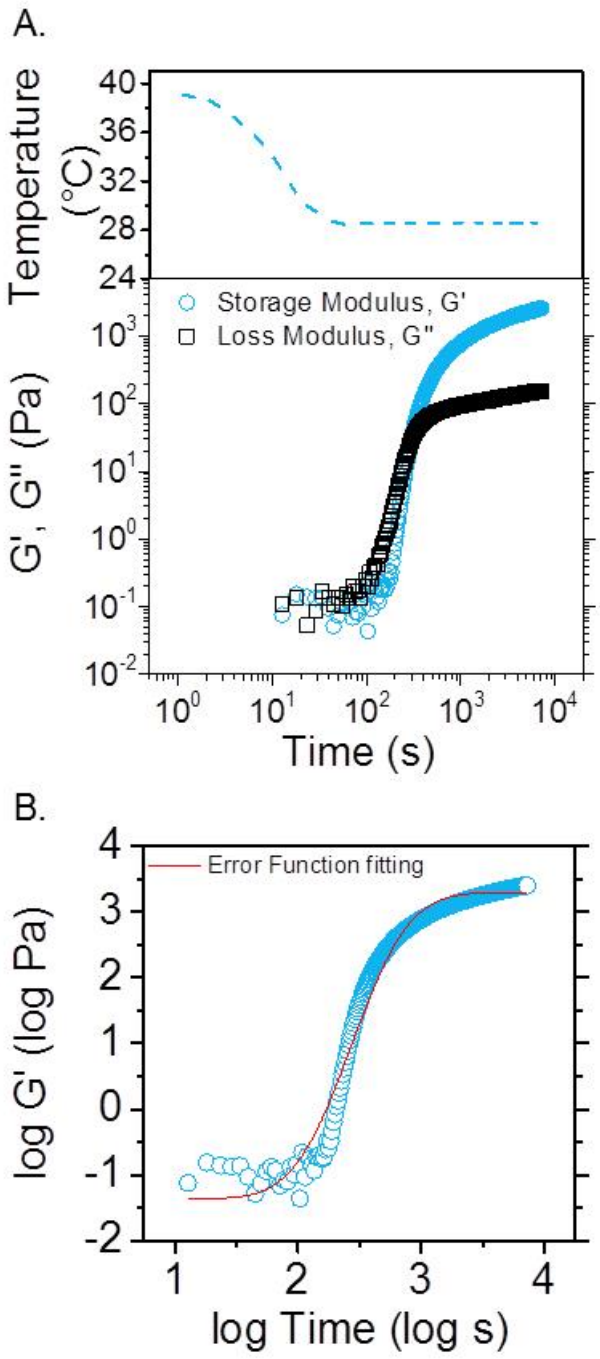

Figure 1. The temperature dependence of the storage and loss moduli. **(A)** After the gel forms and the temperature remains constant, the sample exhibits rheological aging. **(B)** The storage moduli were fit to an error function: log G′= A+ B*erf(C*(log time-D)) where A= 0.97, B=2.33, C=1.91 and D= 2.43. From the fitted D parameter, a characteristic time for gel formation was calculated as approximately 270 seconds.

Small amplitude frequency sweeps for samples quenched from 40°C and subsequently soaked at the desired temperature for 10 min are reported in Figure 2. The experiments were conducted over a period of approximately 4 minutes at 0.1% strain. The thermoreversible gel is very

sensitive to temperature and the critical gel temperature is observed to be 28.8°C using the condition established by Winter and Chambon, in which both moduli have identical frequency dependence [36], which is in good agreement with the temperature of 28.7°C reported previously for this system [17]. The data in Figure 2 shows that, at this critical gel temperature, G′ and G″ are equal and scale with the $\omega^{0.5}$ over several decades of frequency. Based on this data, all subsequent gel aging studies were conducted at 28.6°C, where the sample is a soft gel capable of flowing homogeneously.

From this SAOS data at the reference temperature of 28.6°C, the relaxation dynamics were quantified by fitting to a model based on mode coupling theory (MCT). This theory describes the behavior exhibited in hard sphere colloidal glasses in which a particle is trapped by neighboring particles, forming a 'cage' which hampers its mobility [38]. This theory is associated with a fast relaxation corresponding to diffusive motion within its cage (β relaxation) and a slower relaxation corresponding to particles escaping from the cage (α relaxation). From MCT, the following expression for the storage and loss moduli were developed [39] and adapted for soft particles [40]:

$$G'(\omega) = G_p + G_\sigma \left[\Gamma(1-a') \cos\left(\frac{\pi a'}{2}\right) (\omega t_\beta)^{a'} - B\Gamma(1+b') \cos\left(\frac{\pi b'}{2}\right) (\omega t_\beta)^{-b'} \right] \quad (1)$$

$$G''(\omega) = G_\sigma \left[\Gamma(1-a') \sin\left(\frac{\pi a'}{2}\right) (\omega t_\beta)^{a'} + B\Gamma(1+b') \sin\left(\frac{\pi b'}{2}\right) (\omega t_\beta)^{-b'} \right] + n'_\infty \omega \quad (2)$$

where G_p is the plateau modulus, G_σ is the viscoelastic amplitude, t_β is the β relaxation time and n'_∞ is the high-frequency viscosity. In the absence of a more appropriate theory for adhesive hard spheres, equations 1 and 2 were fit to the linear viscoelastic spectrum at 28.6°C using mode coupling parameters a′=0.301, b′=0.545 and B=0.963, which are recommended for ideal hard spheres [41] (see Figure 2). Following this procedure, the beta relaxation time was determined to be 1.1 s. The beta relaxation time corresponds to diffusive motion within the cage, and is representative of the time required for local bond rearrangement between neighboring particles. Meanwhile, the alpha time is the time required for the gel to flow microscopically and is extrapolated from the model to be of order ~100 s.

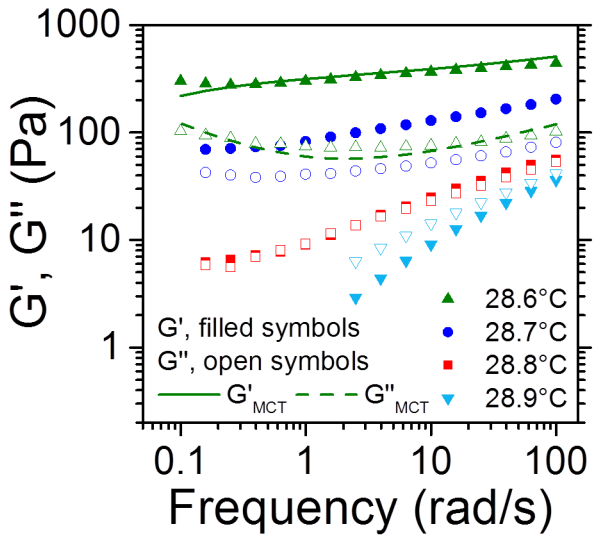

Figure 2. Frequency sweeps at 0.1% strain as a function of temperature. Following the Winter and Chambon criteria, the gel transition temperature is at 28.8°C. All tests were conducted at 28.6°C where the gel is capable of flowing homogeneously. The MCT model fit of G′ (solid line) and G″ (dashed line) reveals a β relaxation time of 1.1 s.

By investigating two different thermal profiles, a reproducible reference state for studying aging in this thermoreversible gel was established. The thermal profiles described earlier briefly consist of 1) directly quenching from the liquid state at 40°C to 28.6°C (i.e., the cooling direction) or 2) quenching from 40°C to 25°C to 28.6°C (i.e., the heating direction). The two different thermal profiles and the corresponding mechanical properties are shown in Figure 3A. The G′ cooling and heating direction curves converge after 4250 seconds, where the storage moduli are within 2% of each other. Therefore, 4250 seconds and 28.6°C was established as the reference state for both quenching protocols. This reference state is approximately 15 times longer than the characteristic time of gel formation described above. At longer times (from the reference state to the conclusion of the two hour experiment), G′ scales with $t^{0.4}$, which agrees with the results for a similar system as reported by Guo et al. [2]. Our results indicate that this scaling is independent of the thermal history during gel formation. Importantly, the approach to the reference state is highly reproducible, as shown in Figure 3B. This data set represents one sample, which was fully rejuvenated by heating to a liquid state and shearing at 40°C between trials; however, slight variability is observed owing to batch-to-batch variation and sample loading.

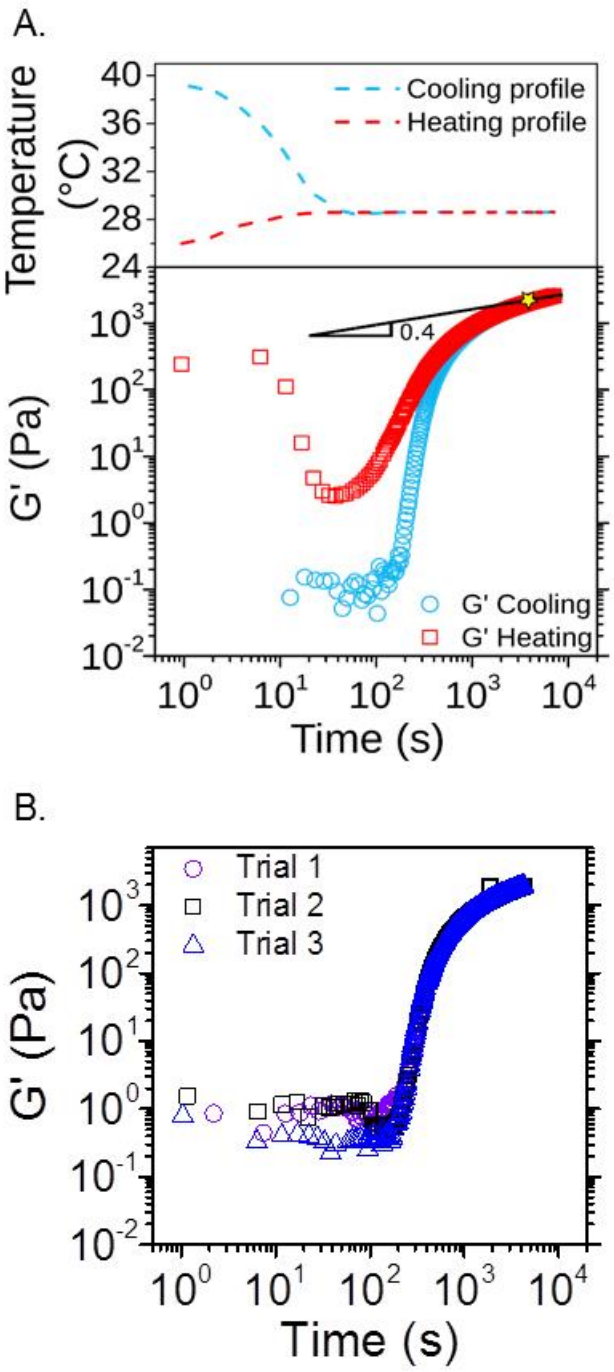

Figure 3. Determination and reproducibility of a reference state during gel aging. **(A)** Temperature profiles and corresponding evolution of the storage and loss moduli. The reference state is denoted by a yellow star and represents the convergence point of the storage moduli from both the heating and cooling directions. At long times, $G' \sim t^{0.4}$, which agrees with the results reported by Guo et al. and is independent of the thermal history during gel formation [2]. **(B)** The approach to the reference state is reproducible. The sample was thermally recycled between trials.

B. Non-linear Rheology of an Aging Thermoreversible Gel

a. Application of Stress to an Aged Gel

The nonlinear rheological response of gels elicited by applying increased levels of shear stress provides insight into the underlying structural dynamics during the gel formation and aging process. Rheological measurements were performed after the sample was aged to its reference state of 28.6°C. After the reference state was reached, creep tests were performed by immediately applying stress to the specimen. The response of the material to different stresses of 25 Pa, 40 Pa, 50 Pa, and 65 Pa was evaluated, where the specimen was rejuvenated and aged before each stress was implemented. The gel responses are displayed in Figure 4A. In all experiments, creep ringing is observed. These short-time oscillations in strain are observed due to the rheometer inertia and sample viscoelasticity, and are therefore expected for a viscoelastic gel tested on a stress-controlled rheometer [42]. At 65 Pa, the sample yields during the experiment. There is a delay of approximately 2 minutes before the onset of flow where stress-driven rearrangements may occur prior to yielding. Identical experiments were performed using the same specimen that was thermally recycled and reformed from the heating direction. Similar responses were observed for both heating and cooling directions, further confirming that the behavior under stress in the aged gel is independent of its thermal history.

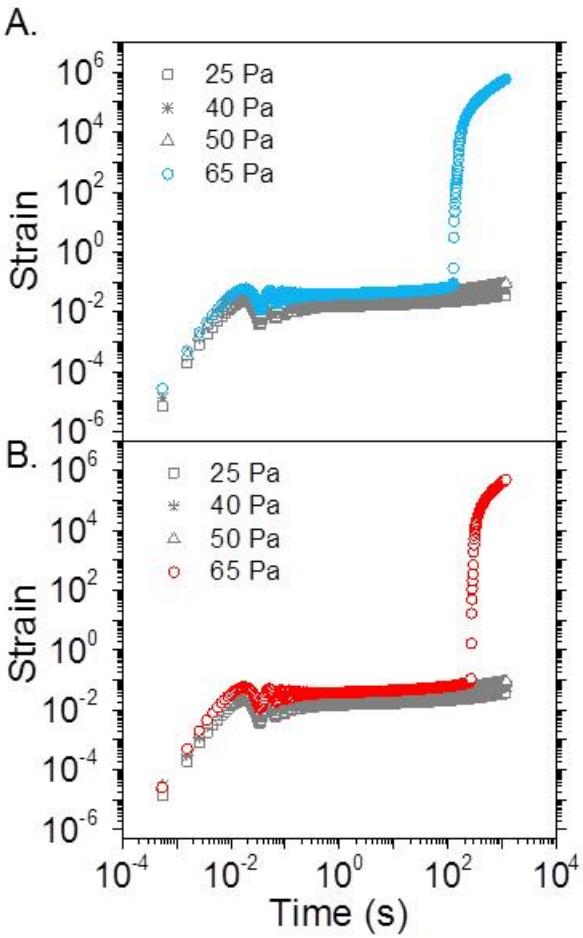

Figure 4. Effect of shear stress on aged gels formed from **(A)** the cooling profile (from 40°C to 28.6°C) and **(B)** from the heating profile (from 25°C to 28.6°C). Creep ringing is observed for all tests, and yielding occurred after 65 Pa was applied. The delay before yielding may indicate stress-induced structural rearrangements in the gel microstructure. Together, these results indicate that the gel response to shear stress in the aged state is independent of its thermal history during gel formation. All data sets were collected from the same specimen that was thermally rejuvenated at 40°C between trials.

Aging in these colloidal gels was further evaluated by interrupting an aging specimen via an applied stress and assessing the impact on the modulus. The specimen was initially thermally rejuvenated and then G′ was monitored using SAOS while the sample aged to the reference state of 4250 seconds at 28.6°C (from the cooling protocol, similar to Figure 3B). A 20 minute creep test was then immediately performed by applying a stress of 0, 25, 40, 50, and 65 Pa. The samples were permitted to recover for 20 additional minutes and the modulus was subsequently monitored using SAOS. No substantial changes in G′ are observed at stress values of 50 Pa and lower. However, for the experiment at 65 Pa, yielding was noted (Figure 4A) and the aging trajectory was considerably altered. In particular, using G′ values to quantify gel "age," the results presented in Figure 5 indicate that the age was reduced by approximately one half after applying 65 Pa. To analyze the post-stress aging further, longer aging studies are presented and interpreted in conjunction with the results of the next study, which are discussed at the end of section b (see Figure 7).

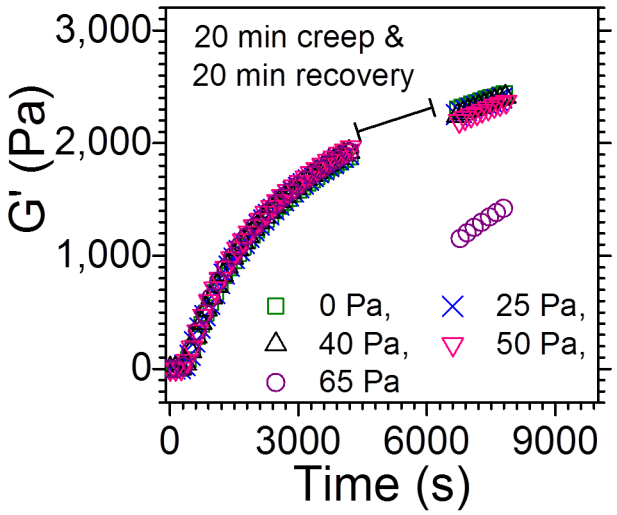

Figure 5. The aging trajectory of one sample that was thermally recycled between tests. In each test, the sample was aged to the reference state of 4250 seconds and shear stresses of 0 Pa, 25 Pa, 40 Pa, 50 Pa and 65 Pa were applied for 20 minutes. The samples recovered for 20 minutes, and aging was monitored for an additional 20 minutes.

b. Application of Stress during Gel Formation

To further explore the stress response of the colloidal gel, stress was applied during gel formation (whereas in the previous section, stress was applied *after* gel formation). Specifically, oscillatory shear stresses of 25 Pa or 40 Pa were applied at 1 Hz until the reference state was reached (at 4250 seconds), followed by SAOS measurements at 0.1% strain and 1 Hz to monitor subsequent structure formation. Gel formation was hindered or suppressed for oscillatory stresses of both 25 and 40 Pa, respectively, as shown in Figure 6 (the 0 Pa continuous SAOS measurement is shown for comparison). While these lower stresses (i.e., < 65 Pa) were insufficient to affect the modulus *after* gel formation (i.e., see Figure 5), the presence of these stresses *during* gel formation significantly affects the formation evolution. In the 40 Pa case, where bulk property measurements indicate that macroscopic gel formation is suppressed under the applied stress, a very rapid rate of G′ evolution is observed when the stress was released. This suggests that some structure was formed in the sample under the applied flow as gel formation occurs more rapidly when the stress was removed.

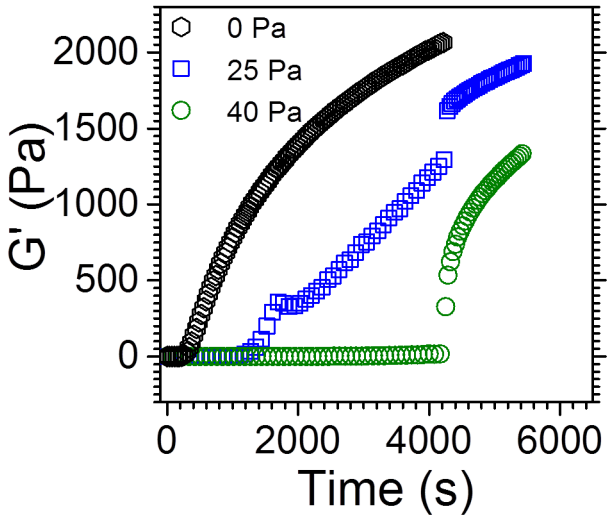

Figure 6. Oscillatory stress applied during gel formation. In each test, the sample was aged to 4250 s, which corresponds to the reference state of the unstressed gels, under oscillatory stresses of 25 Pa and 40 Pa. (The corresponding strain amplitude values under oscillation ranged from 1033% to 1.84% for the 25 Pa experiment and from 1638% to 64.8% for the 40 Pa experiment.) The stress was then released and gel formation was monitored. All measurements were performed at 1 Hz. In the 40 Pa case, bulk property measurements indicate that gel formation was prevented, yet there is a substantial increase in the rate of G′ evolution when compared to the 0 Pa reference case (i.e., 0.1% stain, 1 Hz frequency SAOS experiment), suggesting that the gel microstructure evolved under shear.

The relatively rapid increase in G′ upon cessation of stress as compared to the trial where no stress was applied suggests that the gel microstructure evolved with time under the applied stress, yet we note the same long-term aging behavior in these samples. This effect is evident in Figure 7 where the 40 Pa oscillatory stress data set has been translated in time only to overlay on

the 0 Pa curve. Moreover, longer aging experiments following the application of 65 Pa creep test at the reference state were conducted, which show the same long-time behavior (Figure 7). Specifically, for all three data sets, after the reference state is reached at 4250 seconds, G′ scales with $t^{0.4}$, which is consistent with the aging behavior in Figure 3 and in the work of Guo *et al*. Consequently, these results show that the gel microstructure evolved under shear and the gel eventually ages following similar mechanism of aging as unstressed gels. Thus, gels prepared under different shear conditions in this study will converge to the same long-term behavior. This is further corroborated by microstructural measurements, which are discussed in the following section.

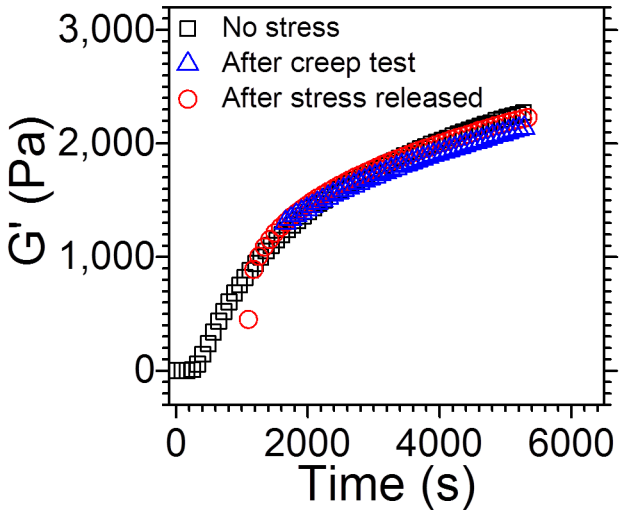

Figure 7: Long-time aging experiments. Data sets shown are (1) "no stress" case where the sample ages under SAOS, (2) "after creep test" case where the gel was subjected to a 20 minute 65 Pa creep tests followed by a 20 minute recovery period prior to aging under SAOS and (3) "after stress released" case where 40 Pa stress was applied to the gel during its formation, and subsequent aging was measured under SAOS after the stress was removed. Time was shifted backwards by 4985 s and 3150 s for the "after creep test" and "after stress released" experiments, respectively to show the same behavior.

C. Microstructural Measurements

Time-resolved Rheo-SANS experiments were conducted to track the evolution of gel microstructure in samples subjected to varied thermal and stress histories. The aging of the specimens was first evaluated in the absence of shear from the cooling and heating direction (Figures 8A and 8B, respectively). In the cooling direction, the sample initially had a liquid-like microstructure that evolved to a microstructure expected for a homogeneous gel [8, 17]. In contrast, gel-like microstructure was initially observed in the heating direction and rapidly evolved to a state consistent with a warmer gel upon heating. The scattering data from the cooling direction are consistent with the particles gradually sampling lower energy states as the gel forms and ages. Moreover, the scattering data collected from the gel formed from the heating direction indicate that the particles sample fewer states as compared to the gel formed from the

cooling direction. This observation is consistent with particles attempting to escape from a deeper energy well achieved by undercooling, and is consistent with the free energy viewpoint of colloidal gel aging.

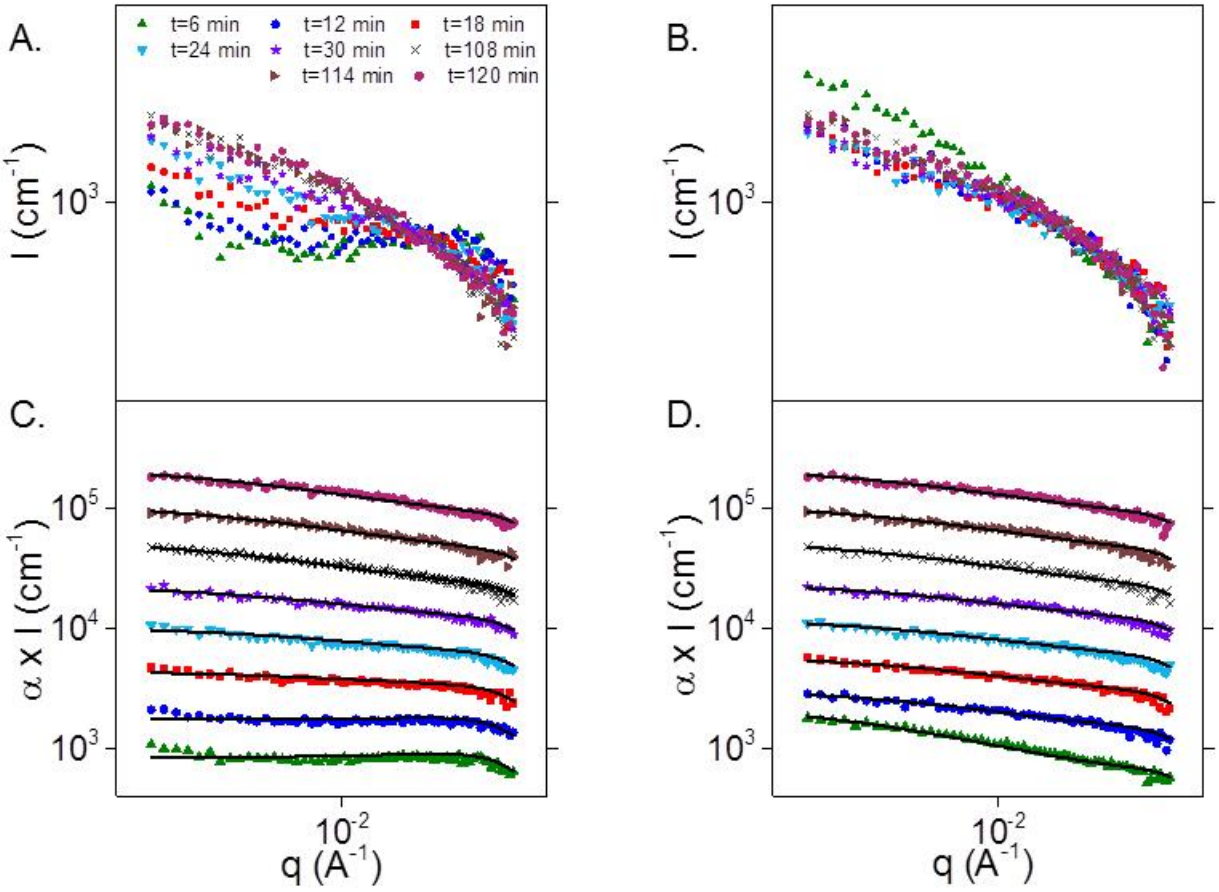

Figure 8: Time-resolved small angle neutron scattering (SANS) data during a two-hour aging experiment. Samples were quenched from the **(A)** cooling direction and **(B)** heating direction. The data were fit to the sticky hard sphere model for the **(C)** cooling direction and **(D)** heating direction. Each subsequent set of intensities was doubled (multiplied by the constant α) from the previous data set to clearly show the fits. Note: the time-resolved data are binned every six minutes and shown on logarithmic scales.

To provide a single parameter quantifying the structure, the scattering data were successfully fit to a liquid state theory model based on the sticky hard sphere (SHS) model (or Baxter model). The Baxter parameter so obtained provides a single parameter that can be used to track how the gel forms and ages, which can be further used to develop a relationship between the microstructure in the gel and corresponding bulk properties. Note that the structures formed from quenching into the gel state are not equilibrium states and instead represent states along an aging trajectory. As such, the Baxter parameters derived from these fits are 'effective' parameters and will converge to the true Baxter parameter for a given temperature as the

structure ages. The fitted results are displayed in Figure 8C and 8D for the cooling and heating data, respectively. Note that scattering curves are displaced in intensity by doubling the intensity sequentially for clarity. Except for the Baxter fit parameter, all other model parameters for octadecyl-coated particles are available from the literature [21] and these parameters are described in the materials and methods section.

To quantify the evolving microstructure in the gel, we introduce λ as the order parameter of the aging structure, which is defined as follows:

$$\lambda = \frac{\tau_{40}^{eq} - \tau^{eff}}{\tau_{40}^{eq} - \tau_{\infty}} \quad (3)$$

where τ_{40}^{eq} is the value of the Baxter parameter in the liquid state at 40°C, τ^{eff} is the value of Baxter fit parameter at each time point and τ_{∞} is the long-time equilibrium Baxter parameter in the gel. By fitting the SHS model to time-resolved SANS data as described above, τ_{40}^{eq}= 0.623 and τ_{∞} ≈0.245.

The evolution of λ in time is displayed in Figures 9A and 9B along with the corresponding storage modulus at the specified time intervals for both the cooling and heating profiles, respectively. Importantly, the monotonic increase in G′ is matched by a monotonic increase in λ (i.e. *aging toward equilibrium*). Further, this quantitative analysis demonstrates that a specific elastic modulus corresponds to a specific microstructure, which is independent of the sample's thermal history (Figure 9C). By plotting log G′ vs. λ for each aging trajectory and, observing an approximately quadratic relationship, we obtain the expression:

$$\log G' = -90.99\,\lambda^2 + 188.16\,\lambda - 94.17 \quad (4)$$

which was fit to both quenching profiles, as shown in Figure 9C. Thus, aging due to local rearrangements leads to microstructures monotonically evolving along a trajectory of ever stronger interactions. This analysis, which is the first of its kind for aging colloidal gels, is consistent with the viewpoint of aging as a trajectory in the free energy landscape, where the microstructure is observed to evolve smoothly towards an equilibrium state with time. Note that aging in polymers is often characterized by a 'fictive' temperature, while previous work on colloids has suggested that aging can result from a time-dependent pair potential (see Guo et al. for a discussion [2]). Our analysis does not support a time-dependent potential, but rather, is a consequence of sampling ever lower free energy states as the sample evolves towards its equilibrium microstructure at a given quench temperature. The structure order parameter is therefore more analogous to the fictive temperature concept invoked for homogenous aging in polymer and colloidal glasses [43]. Moreover, the overshoot of the order parameter in Figure 9B is similar to Kovacs memory effect, which is observed in aging glasses subjected to non-monotonic temperature profiles, and strengthens the case for a connection between λ and the fictive temperature [44].

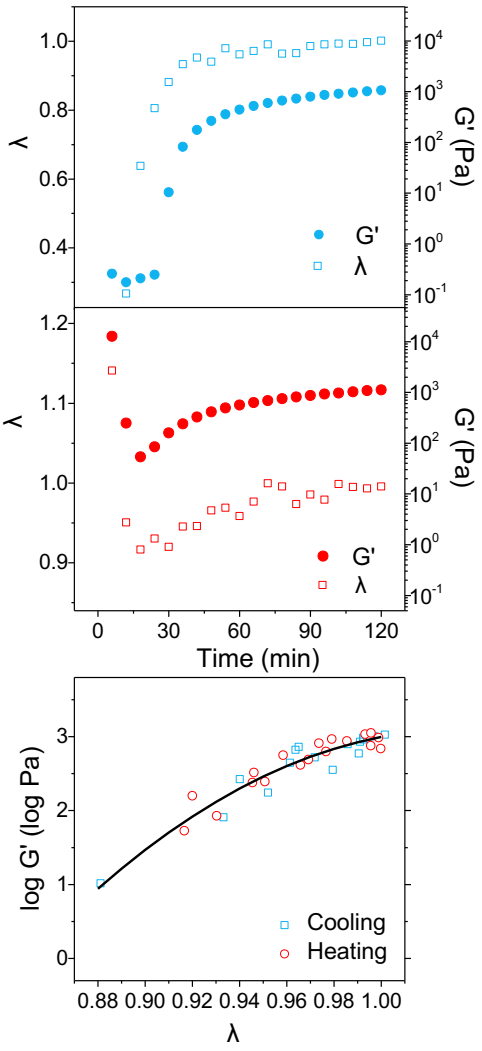

Figure 9: Time-resolved Rheo-SANs measurements. The evolution of the structural parameter λ and G′ as a function of time are shown from the **(A)** cooling direction and **(B)** heating direction. The structural parameter λ was determined from Equation 3 after fitting the sticky hard sphere model to the scattering data at each time point. The plotted value of G′ is an average value of the storage modulus determined from SAOS measurements during the indicated six minute interval. **(C)** The microstructure and storage modulus show a one-to-one correspondence, which is independent of the thermal profile during gel formation. The storage modulus and particle interactions are related by equation 4 over the range of approximately 0.88 to 1.

Microstructural measurements also confirm the choice of reference state, which is consistent with the one-to-one relationship between G′ and microstructure discussed previously. As shown in Figure 10, the scattering data at the reference state for gels quenched from the heating and cooling direction are nearly identical. Both structures are successfully fit to the liquid state theory for a homogeneous AHS colloidal suspension. The Baxter parameters of 0.964 and 0.996 for the cooling and heating direction respectively are well above the critical value for phase

separation. Thus, this result shows that the gel is homogeneous on the particle length scale and the particle interactions are very short-ranged.

To better understand the mechanism by which the system reaches the homogeneous reference state and continues to age, we analyze the mechanical response using mode coupling theory (MCT) to determine the nature of the local particle motion. Within the context of mode coupling theory, the characteristic localization length is the mean-squared displacement associated with local particle motion. Mode coupling theory provides a scaling for homogeneous gels as follows:

$$\frac{G'a^3}{k_BT} = 0.29\frac{\phi a^2}{r_{loc}^2} \tag{5}$$

where r_{loc} is the localization length and a is the particle radius [45]. Using the G′ value corresponding to the reference state of 4250 seconds at 1 Hz reported in Figure 3, r_{loc} was calculated as 3.3 nm. This localization length is on the order of the brush size (reported to be 2.76 nm by Eberle et al. [21]). Thus, particles are bound by contact forces and the elasticity arises from thermal motion on the length scale of the coating responsible for this attraction. This result is consistent with local particle rearrangements as the mechanism of aging. We note that prior researchers studying a similar thermoreversible system observed quantitatively similar localization lengths [19]. The localization length is much larger in repulsive glasses and in depletion gels [9], where the localization length is on the order of the size of the dense, phase-separating clusters [46]. This result strongly supports local particle rearrangements occurring throughout the homogeneous as the mechanism of aging.

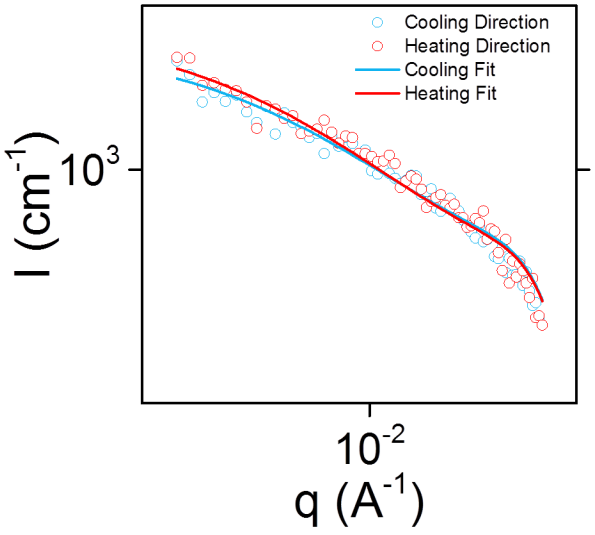

Figure 10: At the reference state, the microstructure of the gels are nearly identical and are independent of the temperature profile during formation. Both data sets are fit to liquid state theory with Baxter parameters of 0.964 and 0.996 for the cooling and heating direction, respectively. Data are shown on logarithmic scales.

Importantly, this analysis suggests that local particle rearrangements and motion are responsible for the mechanical and structural aging under thermal quench. This is clearly distinct from the mechanisms identified in phase separating colloidal gels, where a sequence of particle surface migration, caging, and sequestration in a dense glassy solid have been proposed based on large-scale simulations (see, for example, Zia, Landrum and Russel [27]). Questions remain, however, if this mechanism of local rearrangement extends to aging under an applied shear stress. We extend the study of the gel's stress response by obtaining time-resolved microstructural and rheological measurements while applying oscillatory stress during gel formation by quenching from 40°C. The time-resolved scattering data were binned into 3.5 minute intervals; the first bin and last bin (corresponding to the first 3.5 minutes and the last 3.5 minutes of the 4250 second experiment, respectively) are displayed in Figure 11A with open and closed symbols, respectively. The initial structures are similar and liquid-like, with a correspondingly lower λ values. The microstructures after quenching under stress are characteristic of that of a gel and qualitatively very similar to that observed for purely thermal quenching. Gel formation was observed under oscillatory stresses of 0 Pa, 10 Pa, and 40 Pa. After the stress was released at 4250 s, the initial G' values in these gels were lower than the initial G' value in the unstressed gel (0 Pa), yet the bulk properties in these stressed gels evolved at a faster rate (Figure 11B). Using the relationship developed above quantitatively connecting G' to λ, similar initial mechanical properties were predicted (x markers in Figure 11B) based on λ values from microstructural measurements collected during the final 3.5 minutes of the experiment. The discrepancy between the predicted and measured G' values may be due to both measurement noise from the SANS data collected over short times and expected run-to-run variability. Similarly, from the measured G' values in Figure 11B, corresponding values of λ were calculated, and these predicted fits are indistinguishable from the fit data plotted in Figure 11A. Note that this data are slightly different from that reported in Figure 6 because of differences in the thermal properties of the Rheo-SANS gas-cooled Couette sample environment as compared to the performance of the DHR rheometer with a cone and plate geometry and Peltier. Nevertheless, this sequence of experiments shows that the gel structure evolves under shear in a manner similar to thermal quenching for these homogeneous gels. In this work, we have not tested very large values of the inverse Bingham number, M', such that shear would fundamentally disrupt the gel, as done previously for this system [47]. In other systems where there are substantial heterogeneities in structure and/or dynamics, and where shear may densify the structure, the complex shear history dependence of the microstructure could be expected to lead to a shear history dependence of the mechanical properties that is not equivalent to thermal rejuvenation [48]. We do not observe such effects in our system under the conditions explored.

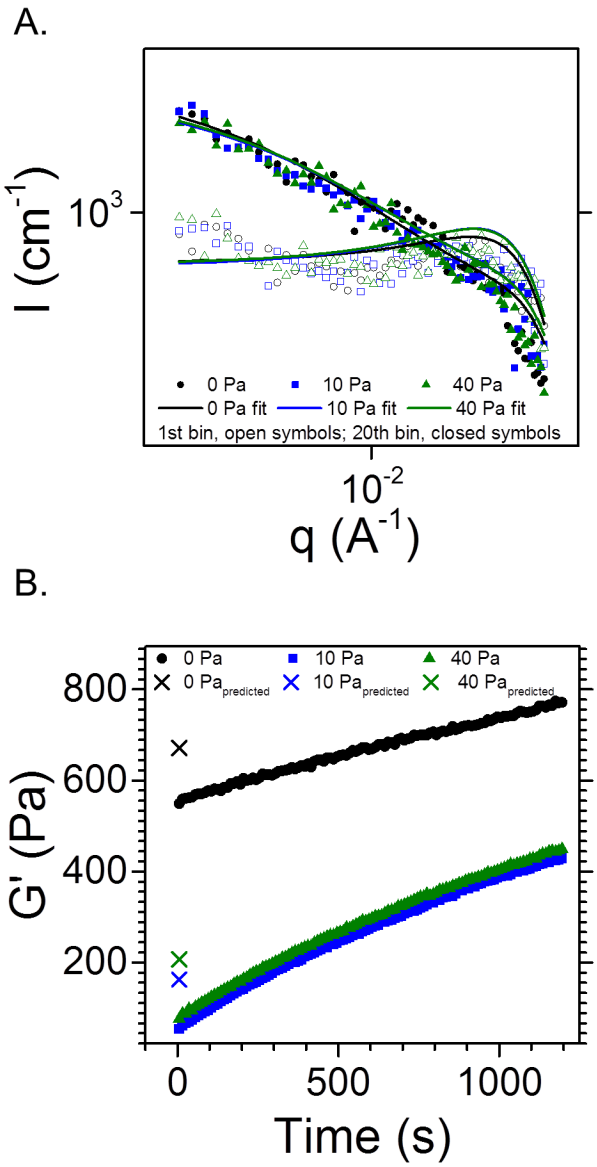

Figure 11: Microstructure and rheology corresponding to a gel quenched under stress. **A.** Time-resolved SANS data were binned into 3.5 minute intervals; the first and last bin corresponds to open and closed symbols, respectively. The microstructure evolved under stress. (The values for the structural parameter λ are as follows: $\lambda_{initial,\ 0\ Pa} \approx 0$, $\lambda_{final,\ 0\ Pa} = 0.976$, $\lambda_{initial,\ 10\ Pa} \approx 0$, $\lambda_{final,\ 10\ Pa} = 0.937$, $\lambda_{initial,\ 40\ Pa} \approx 0$ and $\lambda_{final,\ 40\ Pa} = 0.942$.) Data are shown on logarithmic scales. **B.** Immediately after the stress was released, the initial G′ values were lower in the stressed gels when compared to the unstressed gel (0 Pa), yet the bulk properties in the stressed gels evolved at a faster rate, thereby demonstrating that shear influences how the gel ages.

IV. Summary and Conclusions

In conclusion, we quantitatively relate the bulk rheological properties to the underlying microstructure in an aging, homogeneous, thermoreversible AHS colloidal gel and find a unique,

quantitative relationship irrespective of thermal or shear history over the range of parameters explored. By combining rheology and time-resolved small angle neutron scattering, a reproducible reference state in the continuously aging colloidal gel is established from which stress is applied to probe the gel's response. The rheological behavior after application of stress 1) during gel formation and 2) during gel aging led us to hypothesize that the gel's microstructure develops while under shear during thermal quenching, which is further confirmed by direct microstructural measurements.

The modeling and analysis of concurrent rheological and microstructural measurements provide insight about the colloidal-level motions and interactions responsible for aging. An empirical relationship is developed between an order parameter, which characterizes the distance from equilibrium as determined from scattering measurements of the structure, and the macroscopic property of elastic modulus during gel aging. This empirical relationship enables predicting properties of other rheological experiments from microstructure measurements. For example, we demonstrate that a specific elastic modulus corresponds to a given microstructure, such that the rheological state for a given microstructure is independent of the thermal and shear history of the gel that yielded the given microstructure. Moreover, while the specific microstructure at a given time is dependent on the sample's history, once at a particular microstructure, the sample will quiescently age along the same trajectory regardless of history.

Analysis of the elastic modulus at the reference state with mode coupling theory yields a characteristic localization length of 3.3 nm in the gel, which is comparable to the interaction length between particles in the homogeneous gel. This result is consistent with local particle rearrangements as the mechanism of rheological aging. Indeed SANS measurements of the gel structure confirm that the sample ages homogeneously, and therefore, ages by a mechanism distinct from that observed for phase-separating colloidal gels (e.g., see [27]).

Overall, this work expands our understanding of colloidal gel aging by establishing a quantitative, predictive relationship between the underlying microstructure and bulk mechanical properties, and is consistent with local particle rearrangements as the mechanism of rheological aging. The measurements and analysis support that aging is a trajectory in the free energy landscape, and can ultimately be used to further test and confirm this viewpoint through computational studies. The results of this study may be industrially relevant to products that age on commercially-relevant timescales, such as foods, paints and pharmaceuticals. The approach may also be applicable to other arrested systems, such as metallic glasses, which have been observed to age rheologically in a manner similar to colloidal systems in some respects [49, 50]. Moreover, it is has been suggested that colloids can serve as surrogates for atomic and molecular systems [51, 52]. In particular, the larger size scale of colloidal systems and tunable particle interactions allow for direct measurement of local microstructure and manipulation, respectively, thereby furthering the understanding of complex condensed matter systems and aiding in the design of advanced materials.

V. Acknowledgements

We thank R. Murphy of UD for assistance in obtaining the SANS data in this work. This work was supported by the National Science Foundation Graduate Research Fellowship under Grant No. 1247394 and the Delaware Space Grant College and Fellowship Program under NASA Grant NNX15AI19H. This manuscript was prepared under cooperative agreement 70NANB15H260 from NIST, U.S. Department of Commerce. We acknowledge the support of the National Institute of Standards and Technology, U.S. Department of Commerce, in providing the neutron research facilities used in this work. This work utilized facilities supported in part by the National Science Foundation under Agreement No. DMR-0944772. The statements, findings, conclusions and recommendations are those of the authors and do not necessarily reflect the view of NIST or the U.S. Department of Commerce.

VI. References

[1] Cipelletti, L., and Ramos, L., ‘‘Slow dynamics in glasses, gels and foams,’’ Current Opinion in Colloid & Interface Science **7**, 228-234 (2002).
[2] Guo, H. Y., Ramakrishnan, S., Harden, J. L., and Leheny, R. L., ‘‘Gel formation and aging in weakly attractive nanocolloid suspensions at intermediate concentrations,’’ Journal of Chemical Physics **135** (2011).
[3] Petekidis, G., ‘‘Rheology of colloidal gels,’’ Journal of Rheology **58**, 1085-1087 (2014).
[4] Royall, C. P., Williams, S. R., Ohtsuka, T., and Tanaka, H., ‘‘Direct observation of a local structural mechanism for dynamic arrest,’’ Nature Materials **7**, 556-561 (2008).
[5] Jabbari-Farouji, S., Wegdam, G. H., and Bonn, D., ‘‘Gels and glasses in a single system: Evidence for an intricate free-energy landscape of glassy materials,’’ Physical Review Letters **99** (2007).
[6] Lacks, D. J., and Osborne, M. J., ‘‘Energy landscape picture of overaging and rejuvenation in a sheared glass,’’ Physical Review Letters **93** (2004).
[7] Eberle, A. P. R., and Porcar, L., ‘‘Flow-SANS and Rheo-SANS applied to soft matter,’’ Current Opinion in Colloid & Interface Science **17**, 33-43 (2012).
[8] Eberle, A. P. R., Wagner, N. J., and Castaneda-Priego, R., ‘‘Dynamical Arrest Transition in Nanoparticle Dispersions with Short-Range Interactions,’’ Physical Review Letters **106** (2011).
[9] Zaccarelli, E., ‘‘Colloidal gels: equilibrium and non-equilibrium routes,’’ Journal of Physics-Condensed Matter **19** (2007).
[10] Vanhelden, A. K., Jansen, J. W., and Vrij, A., ‘‘Preparation and Characterization of Spherical Monodisperse Silica Dispersions in Non-Aqueous Solvents,’’ Journal of Colloid and Interface Science **81**, 354-368 (1981).
[11] Chen, M., and Russel, W. B., ‘‘Characteristics of Flocculated Silica Dispersions,’’ Journal of Colloid and Interface Science **141**, 564-577 (1991).
[12] Woutersen, A. T. J. M., and Dekruif, C. G., ‘‘The Rheology of Adhesive Hard-Sphere Dispersions,’’ Journal of Chemical Physics **94**, 5739-5750 (1991).
[13] Grant, M. C., and Russel, W. B., ‘‘Volume-Fraction Dependence of Elastic-Moduli and Transition-Temperatures for Colloidal Silica-Gels,’’ Physical Review E **47**, 2606-2614 (1993).
[14] Rueb, C. J., and Zukoski, C. F., ‘‘Viscoelastic properties of colloidal gels,’’ Journal of Rheology **41**, 197-218 (1997).
[15] Rueb, C. J., and Zukoski, C. F., ‘‘Rheology of suspensions of weakly attractive particles: Approach to gelation,’’ Journal of Rheology **42**, 1451-1476 (1998).

[16] Rouw, P. W., and Dekruif, C. G., ‘‘Adhesive Hard-Sphere Colloidal Dispersions .1. Diffusion-Coefficient as a Function of Well Depth,’’ Journal of Chemical Physics **88**, 7799-7806 (1988).
[17] Eberle, A. P. R., Castaneda-Priego, R., Kim, J. M., and Wagner, N. J., ‘‘Dynamical Arrest, Percolation, Gelation, and Glass Formation in Model Nanoparticle Dispersions with Thermoreversible Adhesive Interactions,’’ Langmuir **28**, 1866-1878 (2012).
[18] Kim, J. M., Eberle, A. P. R., Gurnon, A. K., Porcar, L., and Wagner, N. J., ‘‘The microstructure and rheology of a model, thixotropic nanoparticle gel under steady shear and large amplitude oscillatory shear (LAOS),’’ Journal of Rheology **58**, 1301-1328 (2014).
[19] Ramakrishnan, S., and Zukoski, C. F., ‘‘Microstructure and rheology of thermoreversible nanoparticle gels,’’ Langmuir **22**, 7833-7842 (2006).
[20] Solomon, M. J., and Varadan, P., ‘‘Dynamic structure of thermoreversible colloidal gels of adhesive spheres,’’ Physical Review E **63** (2001).
[21] Eberle, A. P. R., Wagner, N. J., Akgun, B., and Satija, S. K., ‘‘Temperature-Dependent Nanostructure of an End-Tethered Octadecane Brush in Tetradecane and Nanoparticle Phase Behavior,’’ Langmuir **26**, 3003-3007 (2010).
[22] Negi, A. S., Redmon, C. G., Ramakrishnan, S., and Osuji, C. O., ‘‘Viscoelasticity of a colloidal gel during dynamical arrest: Evolution through the critical gel and comparison with a soft colloidal glass,’’ Journal of Rheology **58**, 1557-1579 (2014).
[23] Asakura, S., and Oosawa, F., ‘‘Interaction between Particles Suspended in Solutions of Macromolecules,’’ Journal of Polymer Science **33**, 183-192 (1958).
[24] Poon, W. C. K., Starrs, L., Meeker, S. P., Moussaid, A., Evans, R. M. L., Pusey, P. N., and Robins, M. M., ‘‘Delayed sedimentation of transient gels in colloid-polymer mixtures: dark-field observation, rheology and dynamic light scattering studies,’’ Faraday Discussions **112**, 143-154 (1999).
[25] Buscall, R., Choudhury, T. H., Faers, M. A., Goodwin, J. W., Luckham, P. A., and Partridge, S. J., ‘‘Towards rationalising collapse times for the delayed sedimentation of weakly-aggregated colloidal gels,’’ Soft Matter **5**, 1345-1349 (2009).
[26] Lu, P. J., Zaccarelli, E., Ciulla, F., Schofield, A. B., Sciortino, F., and Weitz, D. A., ‘‘Gelation of particles with short-range attraction,’’ Nature **453**, 499-U4 (2008).
[27] Zia, R. N., Landrum, B. J., and Russel, W. B., ‘‘A micro-mechanical study of coarsening and rheology of colloidal gels: Cage building, cage hopping, and Smoluchowski's ratchet,’’ Journal of Rheology **58**, 1121-1157 (2014).
[28] Verhaegh, N. A. M., Asnaghi, D., Lekkerkerker, H. N. W., Giglio, M., and Cipelletti, L., ‘‘Transient gelation by spinodal decomposition in colloid-polymer mixtures,’’ Physica A **242**, 104-118 (1997).
[29] Zhang, I., Royall, C. P., Faers, M. A., and Bartlett, P., ‘‘Phase separation dynamics in colloid-polymer mixtures: the effect of interaction range,’’ Soft Matter **9**, 2076-2084 (2013).
[30] Koumakis, N., Moghimi, E., Besseling, R., Poon, W. C. K., Brady, J. F., and Petekidis, G., ‘‘Tuning colloidal gels by shear,’’ Soft Matter **11**, 4640-4648 (2015).
[31] Kim, J. M., Fang, J., Eberle, A. P. R., Castaneda-Priego, R., and Wagner, N. J., ‘‘Gel Transition in Adhesive Hard-Sphere Colloidal Dispersions: The Role of Gravitational Effects,’’ Physical Review Letters **110** (2013).
[32] Teece, L. J., Faers, M. A., and Bartlett, P., ‘‘Ageing and collapse in gels with long-range attractions,’’ Soft Matter **7**, 1341-1351 (2011).
[33] Dymond, J. H., and Oye, H. A., ‘‘Viscosity of Selected Liquid N-Alkanes,’’ Journal of Physical and Chemical Reference Data **23**, 41-53 (1994).

[34] Porcar, L., Pozzo, D., Langenbucher, G., Moyer, J., and Butler, P. D., ‘‘Rheo-small-angle neutron scattering at the National Institute of Standards and Technology Center for Neutron Research,’’ Review of Scientific Instruments **82** (2011).
[35] Kline, S. R., ‘‘Reduction and analysis of SANS and USANS data using IGOR Pro,’’ Journal of Applied Crystallography **39**, 895-900 (2006).
[36] Winter, H. H., and Chambon, F., ‘‘Analysis of Linear Viscoelasticity of a Cross-Linking Polymer at the Gel Point,’’ Journal of Rheology **30**, 367-382 (1986).
[37] Valadez-Perez, N. E., Liu, Y., Eberle, A. P. R., Wagner, N. J., and Castaneda-Priego, R., ‘‘Dynamical arrest in adhesive hard-sphere dispersions driven by rigidity percolation,’’ Physical Review E **88** (2013).
[38] Pusey, P. N., and Vanmegen, W., ‘‘Observation of a Glass-Transition in Suspensions of Spherical Colloidal Particles,’’ Physical Review Letters **59**, 2083-2086 (1987).
[39] Mason, T. G., and Weitz, D. A., ‘‘Linear Viscoelasticity of Colloidal Hard-Sphere Suspensions near the Glass-Transition,’’ Physical Review Letters **75**, 2770-2773 (1995).
[40] Helgeson, M. E., Wagner, N. J., and Vlassopoulos, D., ‘‘Viscoelasticity and shear melting of colloidal star polymer glasses,’’ Journal of Rheology **51**, 297-316 (2007).
[41] Gotze, W., and Sjogren, L., ‘‘Beta-Relaxation at the Glass-Transition of Hard-Spherical Colloids,’’ Physical Review A **43**, 5442-5448 (1991).
[42] Baravian, C., and Quemada, D., ‘‘Using instrumental inertia in controlled stress rheometry,’’ Rheologica Acta **37**, 223-233 (1998).
[43] McKenna, G. B., Narita, T., and Lequeux, F., ‘‘Soft colloidal matter: A phenomenological comparison of the aging and mechanical responses with those of molecular glasses,’’ Journal of Rheology **53**, 489-516 (2009).
[44] Kovacs, A. J., Stratton, R. A., and Ferry, J. D., ‘‘Dynamic Mechanical Properties of Polyvinyl Acetate in Shear in Glass Transition Temperature Range,’’ Journal of Physical Chemistry **67**, 152-& (1963).
[45] Chen, Y. L., and Schweizer, K. S., ‘‘Microscopic theory of gelation and elasticity in polymer-particle suspensions,’’ Journal of Chemical Physics **120**, 7212-7222 (2004).
[46] Ramakrishnan, S., Chen, Y. L., Schweizer, K. S., and Zukoski, C. F., ‘‘Elasticity and clustering in concentrated depletion gels,’’ Physical Review E **70** (2004).
[47] Eberle, A. P. R., Martys, N., Porcar, L., Kline, S. R., George, W. L., Kim, J. M., Butler, P. D., and Wagner, N. J., ‘‘Shear viscosity and structural scalings in model adhesive hard-sphere gels,’’ Physical Review E **89** (2014).
[48] Peng, X. G., and McKenna, G. B., ‘‘Comparison of the physical aging behavior of a colloidal glass after shear melting and concentration jumps,’’ Physical Review E **90** (2014).
[49] Siebenburger, M., Ballauff, M., and Voigtmann, T., ‘‘Creep in Colloidal Glasses,’’ Physical Review Letters **108** (2012).
[50] Giordano, V. M., and Ruta, B., ‘‘Unveiling the structural arrangements responsible for the atomic dynamics in metallic glasses during physical aging,’’ Nature Communications **7** (2016).
[51] Leunissen, M. E., Christova, C. G., Hynninen, A. P., Royall, C. P., Campbell, A. I., Imhof, A., Dijkstra, M., van Roij, R., and van Blaaderen, A., ‘‘Ionic colloidal crystals of oppositely charged particles,’’ Nature **437**, 235-240 (2005).
[52] Yethiraj, A., and van Blaaderen, A., ‘‘A colloidal model system with an interaction tunable from hard sphere to soft and dipolar,’’ Nature **421**, 513-517 (2003).